Helix Reversal Motion in Polyisocyanates

Jennifer A. Young* and Robert C. Cook

Lawrence Livermore National Laboratory, Livermore, California 94550

Received September 29, 2000

ABSTRACT: The geometric pathway and energetic barriers associated with the motion of helix reversal sites in poly(methyl isocyanate) have been studied using the conjugate peak refinement algorithm in conjunction with the Merck molecular force field. Motion of the reversal along the chain backbone involves relatively small *net* changes in the torsional angles as a pair of distorted trans and cis bonds reverse their direction of twist. The present study shows that this change occurs by the trans bond passing through its nearby planar low torsional energy conformation to assume an opposite twist. However, the cis bond is prevented from passing through its nearby low torsional energy planar cis conformation by strong nonbonded interactions. It is instead forced to rotate through its trans conformation, thus overcoming two torsional barriers to reach its final cis conformation of opposite twist. The net translation of the reversal down the chain one monomer unit requires crossing three energetic barriers, the highest of which is 17.5 kcal/mol, in reasonable agreement with the 19.6 kcal/mol value determined in recent temperature-dependent NMR studies of poly(2-butylhexyl isocyanate).

I. Introduction

Poly(*n*-alkyl isocyanates) (PICs) have long been known to exist in helical conformations as a result of the competition between electronic and steric factors.[1−4] The helical nature of PICs having chiral alkyl side groups has been demonstrated by several experiments.[5] Chiral side groups cause an energetic preference of one helical sense over the other, giving rise to extraordinarily large optical rotations.[6,7] Due to the cooperative nature of these systems, even the minute energetic effect of an isotope replacement of the α or β hydrogen on the side chain by deuterium produces a large effect. Another important feature is that the optical rotation, and thus relative populations of right (R) and left (L) handed helical sequences, is strongly temperature dependent.[6,7] This is evidence that individual chains contain both right- and left-handed sequences separated by *mobile* helix reversals. PICs with achiral side groups are likewise expected to have mobile helix reversals; however, the equal populations of R- and L-handed helices result in no optical rotation. This degeneracy, however, can be broken by dissolving the polymers in chiral solvent.[8]

Experimental and theoretical techniques have been used to investigate the thermodynamic variables that control the optical activity of polyisocyanates. Lifson et al.[9] have shown that a simple Ising-like model can be used to fit the equilibrium temperature-dependent optical rotation data. The relevant parameters are the energetic preference per monomer for one helical sense over the other and the energetic cost of a reversal. For the chiral system poly((*R*)-1-deuterio-*n*-hexyl isocyanate) (α-PdHIC), the former is found to be about 0.001 kcal/mol while the latter is approximately 4 kcal/mol. In addition, recent temperature-dependent NMR studies have yielded a free energy activation barrier for reversal motion of 19.6 kcal/mol for poly(2-butylhexyl isocyanate) (PBHIC).[10]

Polyisocyanates have been the subject of force field modeling studies for nearly 30 years.[11−14] Initially the interest lay in trying to determine the nature of the helical structure. It is now generally accepted that the helix has a twisted trans/cis structure with the cis bond twisted further out of planarity than the trans bond (see Figure 1 and Table 1). Other authors have examined the reversal conformation, with an eye toward determining its geometry as well as its equilibrium excess energy.[14] This paper focuses on the motion of the reversal, specifically the identification of the multidimensional reaction path traversed as a reversal moves one monomer unit along the chain. Reversal motion effectively converts a monomer from one handedness to the other and may be simplistically represented as

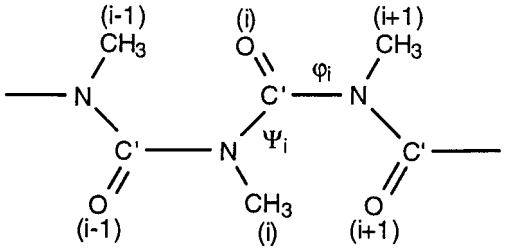

Figure 1. Trans/cis (±180°/0°) structure and numbering system used for poly(methyl isocyanate). The methyl substituents, CH_3, are numbered as single units.

$$...LLLRRRR... \rightarrow ...LLLLRRR...$$

It is important to note that the initial and final states are energetically and geometrically equivalent for polymers with achiral side groups, after allowing for a one monomer, i.e., two bond, translation down the chain. Geometrically this means that a pair of backbone rotational angles, ψ and φ, that were twisted to one side of planarity become twisted to the opposite side of planarity. Clearly the shortest path for this to occur is for the trans and cis bonds to pass *through* their respective planar trans and cis conformations. It will be shown in the following sections that while the trans rotational angle follows this pathway, the cis bond passes through the trans conformer on its way to the opposite side of planarity, overcoming rotational energy barriers along the way.

Computational methods provide a powerful tool for tracking the atomistic level behavior that underlies the

10.1021/ma001695r CCC: $20.00 © 2001 American Chemical Society
Published on Web 04/18/2001

Table 1. Relevant Torsion Angles in the Left- and Right-Handed Chain, the Chain with a Reversal, and the Chain in Which the Reversal Has Moved Down the Chain[a]

	Dihedral Angle									
	Ψ_8	φ_8	Ψ_9	φ_9	Ψ_{10}	φ_{10}	Ψ_{11}	φ_{11}	Ψ_{12}	φ_{12}
Left Helix	-176°	56°	-176°	56°	-176°	56°	-176°	56°	-176°	56°
Right Helix	176°	-56°	176°	-56°	176°	-56°	176°	-56°	176°	-56°
Initial State	-175°	52°	-158°	42°	146°	-73°	180°	-58°	177°	-58°
Final State	-177°	58°	-175°	52°	-158°	42°	146°	-73°	180°	-58°

[a] The position of the reversal is indicated by the bold line.

structural relaxations of polymeric systems. Although molecular dynamics is very useful when applied to processes which occur on short time scales (i.e., having frequencies greater than tens of gigahertz), the limits of statistical sampling imposed by long relaxation times, as observed in the NMR experiments, preclude its use in this study of PIC reversal motion. As in all processes, the energetics of the system dictate its evolution. Therefore, instead of sampling the potential energy surface as is done in molecular dynamics, a search algorithm is employed to determine the lowest energy path across the multidimensional energy surface which connects the initial state and the final state. Specifically, the method of conjugate peak refinement[15] (CPR) is used to mathematically search the complex potential energy surface, identifying saddle points along the path connecting the initial conformation of a chain containing a reversal and the final conformation in which the reversal has moved one monomer unit along the chain.

Poly(methyl isocyanate), PMIC, is chosen for this study because it has been shown that extension of the alkyl side chain beyond its first carbon has relatively little effect on the conformation of the helix.[14] The following sections describe the analysis and the results for PMIC. The simple helix, the geometry of the reversal, and finally the motion of the reversal and the related energy barriers are examined in detail.

II. Methods

Force Field. The Merck molecular force field[16] (MMFF) is used to describe the classical potential energy surface of PMIC. The parameters that describe the inter- and intramolecular energy terms have been obtained using high-quality ab initio calculations and have been validated against experimentally derived data. Partial charges are assigned within the MMFF using the bond increment method. The assignment of charges is as follows: N (−0.42), C′ (0.69), O (−0.57) and for the methyl group C (0.30) and H (0.00).

Nonbonded interactions between the oxygen and methyl substituents are critical in determining not only the equilibrium conformation of PICs but also the reaction path of reversal motion. The partial charges on the hydrogens are zero; therefore, there are no electrostatic interactions between the hydrogens and other atoms. Although the attractive electrostatic interactions between the O and methyl C are important in stabilizing the helix, it will be shown that the van der Waals (vdW) interactions between the oxygens and the hydrogens dictate the ability of atoms to move past each other. MMFF uses a buffered 14−7 potential for the vdW interactions.[17] Specifically, the oxygen−hydrogen interaction of interest here has a well depth of 0.036 kcal/mol at the minimum-energy separation distance of 3.28 Å. The following classification scheme is used to describe these interactions. Strong repulsive vdW interactions are those with energies in excess of 0.40 kcal/mol; this corresponds to O−H separation distances of less than 2.52 Å. This definition is consistent with the minimal contact distances obtained from the Cambridge Crystallographic Data Base.[18] Weak repulsive vdW interactions have separation distances between 2.52 and 3.28 Å and energies between 0.400 and −0.036 kcal/mol.

Rotations along the PMIC backbone are controlled by the C′−N torsional potential. This is 2-fold potential with 17 kcal/mol barriers midway between the planar trans and planar cis states. It may be anticipated that these barriers, which are appropriate for isolated amide linkages, are somewhat higher than the barriers encountered along the delocalized PIC backbone. This has been noted by other authors. In Lifson's molecular mechanics work the rotational barrier was lowered to 12.5 kcal/mol to match the computed and experimentally determined energy cost for a helix reversal.[14] Later ab initio studies have supported the lowering of the barrier by showing that the average torsional barrier for polyisocyanates is lower than that of isolated amides.[19] However, MMFF was found to be effective in matching the experimentally measurable structural and energetic parameters of PICs, as will be discussed shortly. It will also be shown that a lower torsional barrier would have no qualitative effect on the motion of the reversal.

Conjugate Peak Refinement. The CPR algorithm as implemented in CHARMM 26b1[20] is used to identify saddle points along the low-energy pathway that moves the reversal one unit down the chain. This method identifies a series of true saddle points connected to each other through the adiabatic paths that descend from them. A continuous reaction path between initial and final states results. The advantage of CPR is that it requires only initial and final state conformations, the multidimensional potential energy function, and its first derivatives. Other methods commonly require initial guesses of the transition-state structure or the evaluation of the Hessian, the second-derivative matrix.[21−23] The CPR algorithm locates saddle points on the potential energy surface by identifying conformations for which the diagonalized Hessian has one negative eigenvalue while all other eigenvalues are positive. This is done by iteratively (1) determining the maximum energy conformation along a vector, **s**, connecting two states and then (2) minimizing the energy in the conformation subspace conjugate to **s**. Points are added, refined, or removed until all the local maxima along the path are true saddle points. All saddle points in this work have energy gradients of 0.001 kcal/(Å mol) or less. Having determined the saddle points, the other points along the reaction path are relaxed into the minimum-energy path by the method of steepest descents from the saddle points. The progress of the transition between initial and final states is indexed by recording atomic displacements for successive conformations along the path. These distances are then normalized to yield

the reaction path coordinate of the continuous path connecting the initial and final states.

Normal-Mode Analysis. Normal-mode analysis of minimum-energy and saddle-point conformations along the path has been performed. The normal-mode analysis allows the calculation of the Gibbs free energy, which may then be compared to experimental results. The vibrational frequencies, ν_i, are determined by calculating the second-derivative matrix, mass weighting, and then diagonalizing it to obtain the eigenvalues.[24] When in a minimum-energy conformation, six modes corresponding to net translations and rotations have eigenvalues of zero while the remainder are positive. At saddle points one eigenvalue is negative, indicating negative curvature of the potential energy surface along that normal mode. Aside from the six translation and rotation modes the remainder are positive. The normal-mode frequencies are then used to calculate the vibrational thermodynamic functions. Assuming constant pressure and volume, the Gibbs free energy is given by $G = U + G_{vib}$ where U is the internal energy and

$$G_{vib} = \sum_i \left(\frac{h\nu_i}{2} + kT \ln(1 - e^{-h\nu_i/kT}) \right) \quad (1)$$

h is Planck's constant, k is Boltzmann's constant, and T is the temperature.

III. Results

Single-Handed Helix. Chains of PMIC 21 monomer units long were built and their equilibrium conformations obtained by energy minimization. To obtain right- or left-handed helices, the dihedral angles were initially set at $\psi = +170°$ and $\varphi = -50°$ or $\psi = -170°$ and $\varphi = +50°$, respectively. The resulting right- and left-handed helices have the same energy and dihedral angles of opposite sign (see Table 1). The values of $\psi = \pm 176°$ and $\varphi = \mp 56°$ are in general agreement with those obtained by other authors;[14] no effort was made to locate other possible minima.

Central to polyisocyanate helical conformations are the vdW interactions. As anticipated from Figure 1, steric overlap results between O(i) and the hydrogen on R($i - 1$) in the planar trans/cis conformation. A ±56° distortion of the cis bond, φ, lessens the severity of this interaction, resulting in the helical twist of the backbone. Yet a strong repulsive vdW interaction of 0.69 kcal/mol between O(i) and a hydrogen on R($i + 1$) remains. Weak repulsive vdW interactions between O(i) and two of the hydrogens on R($i - 2$) (−0.03 and 0.10 kcal/mol), one hydrogen on R($i - 1$) (0.11 kcal/mol), and one other H on R($i + 1$) (−0.03 kcal/mol) also exist. Therefore, in a single-handed helix each O is surrounded by five hydrogens within the vdW distance of 3.28 Å with a total repulsive vdW energy of 0.84 kcal/mol.

Helix Reversal. A reversal was introduced at the center of the chain by initially setting $\psi_{1-9} = -170°$, $\varphi_{1-9} = +50°$ to give the left-handed segment and $\psi_{10-21} = +170°$, $\varphi_{10-21} = -50°$ to give the right-handed segment. The equilibrium structure was then obtained by minimizing the energy of the entire chain. The same equilibrium helix reversal structure was obtained when two minimized segments of left- and right-handed chains were joined and subsequently relaxed. The torsion angles of the helix containing a reversal, referred to as the initial state, are listed in Table 1. The torsion angles for the final state in which the reversal has moved one monomer unit along the chain are also shown in Table 1. Note that the rotational angle distortions are largely confined to the repeat units on either side of the reversal point. While single-handed helices yield perfectly straight rodlike structures, the introduction of a reversal results in an angle of 133° between the right- and left-handed segments.

The energy excess for the chain with a reversal over that of a single handed helix, ΔG_r, was computed by incorporating both the internal and vibrational energy contributions as described in the previous section. The calculated free energy excess, ΔG_r, is 2.92 kcal/mol for PMIC, somewhat less than the experimentally determined value of about 4 kcal/mol for α-PdHIC.[9] The difference in these values may be partly due to the difference in the size of the substituent groups. The major contribution to the computed ΔG_r comes from the internal energy, ΔU, which is 2.74 kcal/mol. Analysis shows that the distortion of the dihedral angles in the vicinity of the reversal makes the major contribution to ΔU, 1.68 kcal/mol. Angle bending and electrostatic interactions also contribute 0.98 and 0.72 kcal/mol, respectively. The increase in angle bend energy is due to several angle distortions of 1°−3° in the vicinity of the reversal. The vibrational contribution to the total energy is small, 0.18 kcal/mol.

Interestingly, the total vdW energy *decreases* by 0.70 kcal/mol upon going from the single-handed helix to one with a reversal. Most of this decrease is accounted for by the repulsive vdW interactions between oxygens and hydrogens in the region of the reversal (see Table 2). For example, O(6), which resides in the left-handed helix segment, is within the minimum vdW distance of two hydrogens on methyl four, R(4), one on R(5), and two on R(7) as previously described. Therefore, the vdW interaction energy between O(6) and the hydrogens which surround it is 0.84 kcal/mol, representative of a single-handed helix. The decrease in the vdW energy for chains with reversals is primarily due to the alleviation of the close contacts between O(8)−R(9) and O(9)−R(10) in the vicinity of the initial reversal state. These atoms lie on the exterior of the bend, thereby avoiding the packing constraints felt by other atoms along the chain. The remainder of the 0.70 kcal/mol difference in the vdW energy is distributed among other interactions along the chain.

Reversal Motion. The propagation of the reversal one unit down the chain involves the movement of R(9) from the distorted reversal region into the left-handed helical segment and R(11) from the right-handed segment into the reversal region. Complex changes in both the nonbonded interactions and backbone dihedral angles are necessary for these changes to occur. Table 2, which shows the vdW interactions in the initial and final states, can be used to examine the required changes in the nonbonded interactions. Note that the environment seen by O(i) in the initial state is the same as that seen by O($i + 1$) in the final state after the reversal has moved to the right. Reversal motion requires that O(11) distance itself from R(8) and instead come into contact with R(9) while simultaneously O(12) loses contact with two hydrogens on R(10) and picks up one vdW interaction with R(9). The magnitudes of the O(i)/R($i + 1$) interactions near the reversal must also change. Not only are changes in the magnitudes of the vdW interactions important but also the relative positions of atoms in the region of the reversal. For example, R(10), which is initially situated on one side of O(11), must move to the other side in the final state. Likewise,

Table 2. Repulsive vdW Energies in kcal/mol between the Oxygen of Residue *i*, O(*i*), and Individual Hydrogens on Methyl *i*, R(*i*), for the Initial and Final State Chain[a]

	O(i)									
initial	6	7	8	9	10	11	12	13	14	15
final	7	8	9	10	11	12	13	14	15	16
R(i-3)						0.17				
R(i-2)	-0.03 0.10	-0.03 0.08	-0.07 0.11	-0.03 0.11	 -0.02		-0.03 0.18	-0.03 0.11	-0.03 0.10	-0.03 0.10
R(i-1)	0.11	0.11	0.10	0.02	-0.02 0.32	0.17	0.11	0.11	0.11	0.11
R(i+1)	-0.03 0.69	-0.03 0.80	0.09 0.28	0.06 0.36	-0.03 0.50	-0.03 0.69	-0.03 0.69	-0.03 0.69	-0.03 0.69	-0.03 0.69
Total	0.84	0.93	0.51	0.52	0.75	1.00	0.92	0.85	0.84	0.84
ΔvdW	0.00	+0.09	-0.33	-0.32	-0.09	+0.16	+0.08	+0.01	0.00	0.00

[a] The bold vertical line indicates the reversal position. The difference in vdW energy relative to an oxygen in a single-handed helix is reported.

the relative positions of O(12) and R(9) must change upon reversal propagation. These changes in the relative positions may be achieved in one of two fashions. The atoms may push directly past each other, or they may avoid direct contact by rotating in opposite directions to achieve their final positions. The question of how the methyl groups reposition themselves in relation to the oxygen atoms is central in determining the pathway of reversal motion in PIC chains.

Reversal motion requires that two dihedral angles move to the opposite side of planarity. Specifically, Table 1 shows that ψ_{10} must change from +146° to −158° and φ_{10} from −73° to +42° for the reversal to move. As discussed earlier, it might be anticipated that this transition occurs by ψ_{10} passing through the dihedral energy minimum at 180° (trans) while φ_{10} passes through the minimum at 0° (cis). The reversal would then be said to move via a trans/cis transition.

Surprisingly, analysis of the conformations along the low-energy reaction pathway of PMIC reveals a trans/trans transition instead of a trans/cis transition (see Figure 2). Although ψ_{10} approaches and crosses the rotational barrier at +90°, its movement to the other side of planarity ultimately occurs by passing through the trans conformation at 180°. Meanwhile, φ_{10} rotates 245° overcoming the energy barriers at ±90° in moving to the other side of planarity. φ_{10} thereby passes through the trans conformation during reversal propagation. Figure 3 demonstrates that reversal motion is a complex process involving the coupled motions of other torsional angles, specifically ψ_{11} and φ_{11}. Note that ψ_{11} also

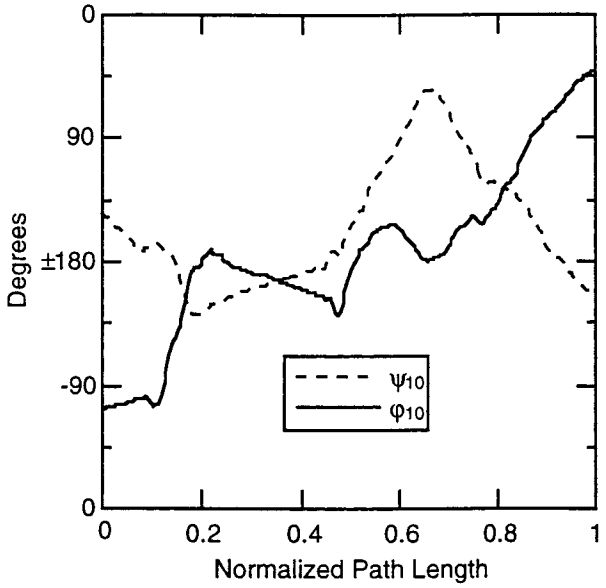

Figure 2. Evolution of dihedral angles ψ_{10} and φ_{10} along the reaction pathway is displayed. The trans/trans transition is observed halfway along the path. Note that cis = 0° and trans = 180°.

traverses an energy barrier at 90° during reversal propagation. Dihedral angles more distant from the reversal site undergo negligible torsional changes during reversal motion, confirming that a 21-mer is a sufficiently large representation of the chain. The

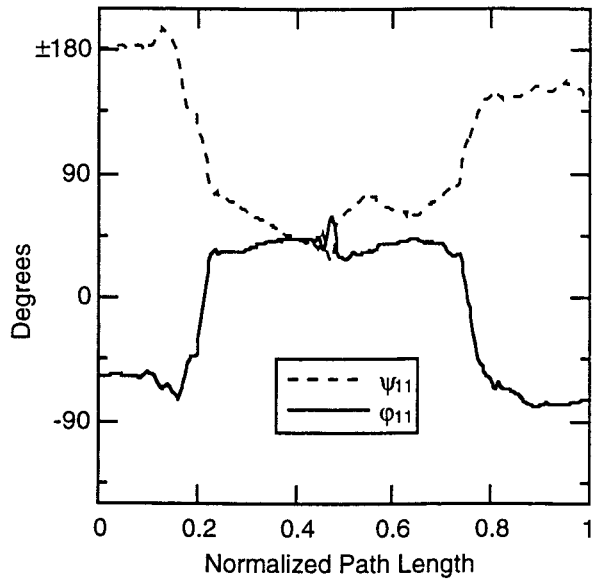

Figure 3. Dihedrals ψ_{11} and φ_{11} also undergo large rotations as the reversal propagates along the chain. Note that ψ_{11} temporarily crosses the rotational energy barrier at 90°.

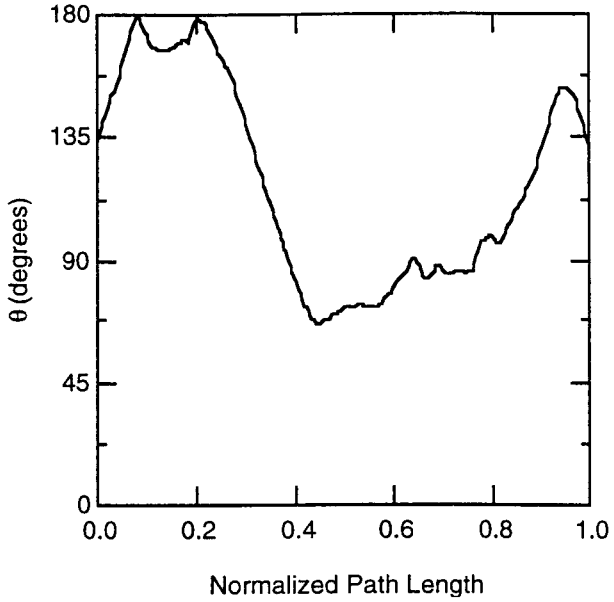

Figure 4. Kink angle of the chain undergoes large changes as the reversal moves.

reasons that φ_{10} rotates through the trans conformation, thus passing over the energy barrier for backbone rotation, will be presented in the Discussion.

The overall shape of the chain is monitored by tracking the angle between right- and left-handed helical segments. As seen in Figure 4, the chain undergoes a breathing motion as the reversal moves along the chain. Initially the chain straightens and then bends to 65° before finally returning to 133°. The severe bend in the chain midway through the transition effectively distances atom O(11) from R(10) and atom O(12) from R(9). This allows these atoms to reposition themselves without directly passing by each other, thus avoiding highly repulsive vdW interactions.

The reaction pathway for reversal propagation reveals three distinct transition states (see the top of Figure 5). Table 3 shows the energies of the saddle-point and local minimum-energy conformations relative to the

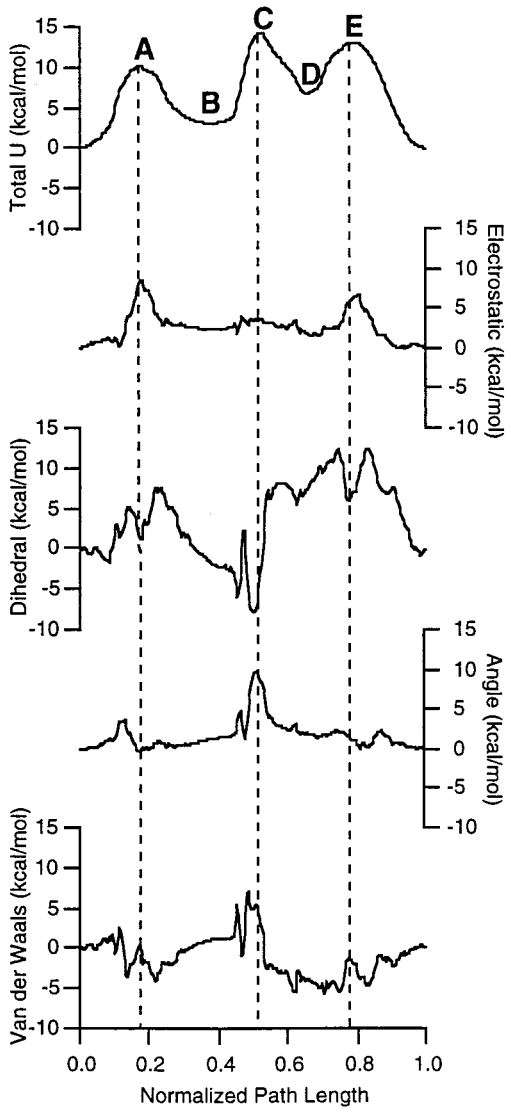

Figure 5. At the top the energy profile along the reaction pathway of helix reversal motion is shown. The electrostatic, dihedral, angle, and vdW contributions are displayed below. The positions of conformations A−E along the path are noted.

Table 3. Thermodynamic Contributions to the Total Energies of the Saddle-Point and Local Minimum-Energy Conformations[a]

	conformation				
	A	B	C	D	E
ΔU	10.20	5.81	14.22	9.51	12.96
ΔG_{vib}	1.82	0.61	3.33	0.33	1.77
ΔG	12.02	6.42	17.55	9.84	14.73

[a] All energies are relative to the initial state and are given in units of kcal/mol at $T = 413$ K.

initial state. Note that the vibrational component is larger at the saddle points (A, C, and E) than at the minima (B and D). This is due to the decrease in entropy in moving from a minimum-energy conformation to a saddle-point conformation. The calculated free energy barriers for reversal propagation reveal that saddle point C is the rate-determining step with $\Delta G^* = 17.55$ kcal/mol at 413 K. This is in good agreement with the NMR studies that give a barrier height of 19.6 kcal/mol for PBHIC at the same temperature.[10]

Decomposing the total internal energy of the PMIC chain along the reaction path reveals the energetics

Table 4. Repulsive vdW Energies between the Oxygen of Residue *i*, O(*i*), and Hydrogens on Methyl *i*, R(*i*), for the Trans/Trans Conformation[a]

	O(*i*)									
	6	7	8	9	10	11	12	13	14	15
R($i-2$)	−0.03	−0.03	−0.03	−0.03	−0.01		−0.02		−0.03	−0.03
	0.10	0.09	0.10	0.10	0.12		0.04		0.16	0.10
R($i-1$)	0.11	0.11	0.10	0.11	0.06			0.15	0.11	0.11
R(*i*)						0.16				
						0.34				
R($i+1$)	−0.03	−0.03	0.00	0.16		0.04	−0.02	−0.03	−0.03	−0.03
	0.69	0.73	0.45	0.45		0.43	0.50	0.69	0.69	0.69
total	0.84	0.87	0.62	0.79	0.17	0.97	0.50	0.81	0.89	0.84
ΔvdW	0.00	+0.03	−0.22	−0.05	−0.67	+0.13	−0.34	−0.03	+0.05	0.00

[a] The difference in vdW energy relative to an oxygen in a single-handed helix is reported. All energies are in kcal/mol.

Table 5. Repulsive vdW Energies between the Oxygen of Residue *i*, O(*i*), and Hydrogens on Methyl *i*, R(*i*), for the Trans/Cis Conformation[a]

	O(*i*)									
	6	7	8	9	10	11	12	13	14	15
R($i-3$)							0.15			
							0.42			
R($i-2$)	−0.03	−0.03	−0.03	−0.03	−0.02			−0.02	−0.03	−0.03
	0.10	0.09	0.09	0.10	0.12			0.11	0.10	0.10
R($i-1$)	0.11	0.11	0.11	0.12	0.19	0.00		0.04	0.11	0.11
						0.12				
R(*i*)						−0.03				
						0.13				
R($i+1$)	−0.03	−0.03	0.00	−0.03	0.12	0.04	−0.03	−0.03	−0.03	−0.03
	0.69	0.73	0.85	1.14	0.36	0.40	0.73	0.69	0.69	0.69
total	0.84	0.87	1.02	1.30	0.77	0.66	1.25	0.79	0.84	0.84
ΔvdW	0.00	+0.03	+0.18	+0.46	−0.07	−0.18	+0.43	−0.05	0.00	0.00

[a] The difference in vdW energy relative to an oxygen in a single-handed helix is reported. All energies are in kcal/mol.

involved in reversal propagation. Figure 5 shows the contributions that electrostatic, dihedral rotation, angle bending, and vdW interactions make along the path. Although the complex and interrelated nature of the energy profiles does not always allow a simple isolation of their atomistic origins, the following observations may be made. The energy barrier at conformation A has two sources. First, the two subpeaks in the dihedral energy are due to φ_{10} and ψ_{11} passing over the dihedral energy barrier at 90°. The vdW energy mirrors the dihedral energy because conformations that minimize the dihedral energy simultaneously maximize the repulsive vdW interactions and vice versa. The peak in the electrostatic energy at A is due to the loss of favorable interactions as the negatively charged O(11) rotates away from the positively charged C and C′ atoms. Favorable electrostatic interactions are then regained while ψ_{11} and φ_{11} remain in their metastable positions around 45° following point A.

Barrier C, the rate-determining step, is due to the movement of R(11) past R(10) and O(11). The temporary peak in the dihedral energy preceding C is due to several dihedral angles rotating approximately 20° closer to the 90° barrier, thereby allowing atoms on the exterior of the bend to reposition themselves. At conformation C, ψ_{10} and φ_{10} pass through the planar trans/trans conformation, resulting in the minimum in the dihedral energy. The corresponding peak in the vdW energy is due to the close packing of R(11) against R(10) and O(11). The large angle bend contribution is due to multiple angle distortions of 2° or 3° as the aforementioned atoms move past each other. The sharp increase in dihedral energy after C is due to torsional distortion as a result of R(11) moving past R(10) and O(11) and the movement of ψ_{10} toward the barrier at 90°.

Barrier E has many characteristics in common with barrier A. The peaks in the dihedral energy are due to ψ_{10}, φ_{10}, and ψ_{11} passing over torsional barriers at 90°. The peak in the electrostatic energy is due to O(11) losing the favorable interactions it had established while ψ_{11} and φ_{11} remained around 45°. Favorable electrostatic interactions with the backbone atoms are then regained as O(11) assumes its final position relative to R(11).

IV. Discussion

The question raised by these results is why does φ_{10} pass through the trans state instead of the cis state in going from −73° to 42°? The answer lies in the balance between backbone rigidity and steric interactions.

To compare the possibility of trans/trans and trans/cis transitions, the following procedure was employed. The trans/trans transition state conformation was obtained by setting $\psi_{10} = 180°$ and $\varphi_{10} = 180°$ in a chain with a reversal and then minimizing the energy of the remainder of the structure. The resulting conformation is a good representation of the trans/trans transition state conformation that arises about halfway along the reaction path. Similarly, a trial trans/cis transition state conformation was obtained by setting $\psi_{10} = 180°$ and $\varphi_{10} = 0°$ and minimizing the energy. The important O−H vdW interactions for the trans/trans and trans/cis conformations are listed in Tables 4 and 5. The O−H vdW energy relative to the single-handed helix is seen to decrease by 1.10 kcal/mol in the trans/trans conformation while increasing by 0.80 kcal/mol in the trans/cis conformation The specific packing of the atoms in the trans/cis conformation will now be examined in detail to see how this conformation prevents reversal motion.

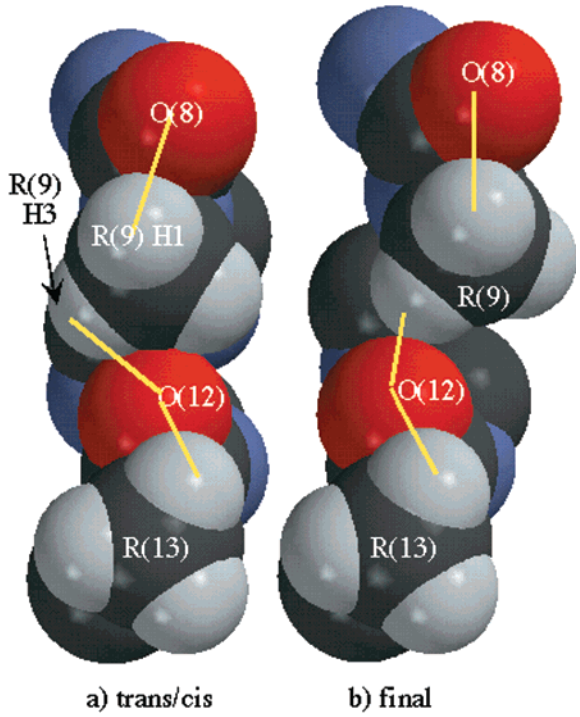

Figure 6. (a) Packing of atoms in the trans/cis conformation creates an impassible barrier to reversal propagation. (b) Packing of atoms in the final conformation, i.e., after the reversal has moved. Yellow lines highlight the important vdW interactions.

Although propagation of the reversal through trans/cis conformation would allow ψ_{10} and φ_{10} to directly pass to the other side of planarity, this reaction path would require that O(12) push directly past R(9) and O(11) push past R(10). Figure 6a focuses on the vdW interactions which limit the ability of R(9) to move past O(12) on its way to assuming the final conformation, shown in Figure 6b. The movement of R(9) past O(12) via a trans/cis conformation would most likely be initiated by rotation of R(9), specifically the rotation of the hydrogens on this methyl past O(12). Counterclockwise rotation of R(9) would severely increase the vdW interaction energy between H3 and O(12). This is due largely to the inability of O(12) to move out of the way of H3 because of its strong repulsive interaction with R(13). Likewise, clockwise rotation of R(9) is restricted due to the strong repulsive interaction between H1 of R(9) and O(8).

The other reason the trans/cis transformation seems unlikely involves the movement of O(11) past R(10). As seen in Table 5, the trans/cis conformation results in 1.14 kcal/mol vdW interaction between these atoms. While the actual extent of the vdW interaction between these atoms during a trans/cis transition might be somewhat less, the requirement that they directly pass each other indicates that the energy barrier will be sizable. In short, the vdW interactions encountered in the trans/cis conformation create an impassible vdW barrier, preventing reversal motion via this pathway.

VdW interactions are also central to shaping the trans/trans low-energy pathway. As seen in Figure 5, the rate-determining step in reversal propagation, saddle point C, is dominated by vdW interactions and related angle distortions. The vdW interactions are due to R(11) moving past R(10) and O(11) on the exterior of the bent chain. Unlike the trans/cis transition outlined above, the trans/trans reaction pathway repositions O(11) relative to R(10) and O(12) relative to R(9), not by pushing them *directly* past each other, but instead by rotating the atoms away from each other to their new positions. This is possible due to the 245° rotation of φ_{10} and the coupled rotations of ψ_{11} and φ_{11}. It is these rotations which cause the large bend in the overall PMIC chain structure during reversal motion (see Figure 4). The saddle points at A and E are due to dihedral rotations over barriers and the electrostatic interactions that accompany them. Specifically, Figures 2 and 3 show that at these points φ_{10} and ψ_{11} overcome the 17 kcal/mol rotational barrier. Therefore, one can conclude that lowering the C′−N backbone rotational barrier would simply lower the energy barriers at A and E, having little effect on the barrier at C.

Although energetically and conformationally complex, helix reversal motion along the poly(methylisocyanate) chain has been shown to occur via a trans/trans pathway. Evidence suggests that this result for poly(methyl isocyanate), the polyisocyanate with the simplest of alkyl side groups, is valid for polyisocyanates in general. The reasons are as follows. First, the computed values of key parameters such as the energy excess of a chain with a reversal over that of a single-handed helix and the calculated free energy barrier for reversal propagation are in qualitative agreement with experimental results for other polyisocyanates. Second, previous modeling work has shown that larger alkyl side groups have relatively little effect on the helix.[14] Finally, we have presented arguments that altering the force field by lowering the torsional barrier to account for backbone electron delocalization would still result in a trans/trans pathway for helix reversal motion. Nonbonded interactions rather than the backbone torsional potential determine the reaction pathway for reversal motion in polyisocyanates.

Acknowledgment. This work was performed under the auspices of the U.S. Department of Energy by the University of California Lawrence Livermore National Laboratory under Contract W-7405-Eng-48.

References and Notes

(1) Shmueli, U.; Traub, W.; Rosenheck, K. *J. Polym. Sci, Part A-2* **1969**, *7*, 515.
(2) Berger, M. N.; Tidswell, B. M. *J. Polym. Sci., Polym. Symp.* **1973**, *42*, 1063.
(3) Bur, A. J.; Fetters, L. J. *Chem. Rev.* **1976**, *76*, 727.
(4) Cook, R.; Johnson, R. D.; Wade, C. G.; O'Leary, D. J.; Munoz, B.; Green, M. M. *Macromolecules* **1990**, *23*, 3454.
(5) Green, M. M.; Peterson, N. C.; Sato, T.; Teramoto, A.; Cook, R.; Lifson, S. *Science* **1995**, *268*, 1860.
(6) Green, M. M.; Andreola, C.; Munoz, B.; Reidy, M. P.; Zero, K. *J. Am. Chem. Soc.* **1988**, *110*, 4063.
(7) Green, M. M.; Reidy, M. P.; Johnson, R. J.; Darling, G.; O'Leary, D. J.; Willson, G. *J. Am. Chem. Soc.* **1989**, *111*, 6452.
(8) Green, M. M.; Khatri, C.; Peterson, N. C. *J. Am. Chem. Soc.* **1993**, *115*, 4941.
(9) Lifson, S.; Andreola, C.; Peterson, N. C.; Green, M. M. *J. Am. Chem. Soc.* **1989**, *111*, 8850.
(10) Ute, K.; Fukunishi, Y.; Jha, S. K.; Cheon, K.; Munoz, B.; Hatada, K.; Green, M. M. *Macromolecules* **1999**, *32*, 1304.
(11) Troxell, T. C.; Scheraga, H. A. *Macromolecules* **1971**, *4*, 528.
(12) Han, C. C.-C.; Yu, H. *Polym. Prepr. (Am. Chem. Soc., Div. Polym. Chem.)* **1973**, *14*, 121.
(13) Tonelli, A. E. *Macromolecules* **1974**, *7*, 628.
(14) Lifson, S.; Felder, C. E.; Green, M. M. *Macromolecules* **1992**, *25*, 4142.

(15) Fischer, S.; Karplus, M. *Chem. Phys. Lett.* **1992**, *194*, 252.
(16) Halgren, T. A. *J. Comput. Chem.* **1996**, *17*, 490.
(17) Halgren, T. A. *J. Comput. Chem.* **1996**, *17*, 520.
(18) Allen, F. H.; Bellard, S.; Brice, M. D.; Cartwright, B. A.; Doubleday, A.; Higgs, H.; Hummelink, T.; Hummelink-Peters, B. G.; Kennard, O.; Motherwell, W. D. S.; Rodgers, J. R.; Watson, D. G. *Acta Crystallogr., Sect. B* **1979**, *35*, 2331.
(19) Raos, G.; Bielli, P.; Tornaghi, E. *Int. J. Quantum Chem.* **1999**, *74*, 249.
(20) Brooks, B. R.; Bruccoleri, R. E.; Olafson, B. D.; States, D. J.; Swaminathan, S.; Karplus, M. *J. Comput. Chem.* **1983**, *4*, 187.
(21) Bell, S.; Crighton, J. *J. Chem. Phys.* **1984**, *80*, 2464.
(22) Muller, K.; Brown, L. D. *Theor. Chim. Acta* **1979**, *53*, 75.
(23) Ulitsky, A.; Elber, R. *J. Chem. Phys.* **1990**, *92*, 1510.
(24) Wilson, E. B.; Decius, J. C.; Cross, P. C. *Molecular Vibrations*; McGraw-Hill: New York, 1955.

MA001695R